Vision-based Lane Detection for Passenger Cars: Configuration Aspects

Kunsoo Huh, Jaehak Park, Daegun Hong, Dongil 'Dan' Cho, *Member, IEEE*, and Jahng Hyon Park

Abstract— **Vision-based lane sensing systems require accurate and robust sensing performance in lane detection. Besides, there exists trade-off between the computational burden and processor cost, which should be considered for implementing the systems in passenger cars. In this paper, a stereo vision-based lane detection system is developed with considering sensor configuration aspects. An inverse perspective mapping method is formulated based on the relative correspondence between the left and right cameras so that the 3-dimensional road geometry can be reconstructed in a robust manner. A new monitoring model for estimating the road geometry parameters is constructed to reduce the number of the measured signals. The selection of the sensor configuration and specifications is investigated by utilizing the characteristics of standard highways. Based on the sensor configurations, it is shown that appropriate sensing region on the camera image coordinate can be determined. The proposed system is implemented on a passenger car and verified experimentally.**

I. Introduction

LANE sensing systems based on vision sensors are regarded promising because they require little infrastructure on the highway except clear lane markers. These systems are believed to inform the driver of the possible lane departure accident and, if necessary, to override the driver's steering command. However, the feasibility of these systems in passenger car requires accurate and robust sensing performance in lane detection. In addition, trade-off between the computational burden and processor cost should be considered for the real-time image processing in passenger cars.

The image processing algorithms are basically composed of image acquisition process and inverse perspective mapping. The image acquisition process can be considered as a transform from the 3D world space to the 2D image plane. Conversely, inverse perspective mapping is an inverse transform from the 2D image plane back to the 3D world space by removing the perspective effect. The inverse perspective mapping is usually indeterminate because some of the 3D information is lost during the image acquisition. To overcome these limitations, various image processing algorithms [1-13, *et al.*] have been developed for vision cameras. For instance, 3D lane edge is detected solely based on the vision image [1-4, *et al.*], but the image processing algorithms can be very complicated. In order to reduce the computational burden and to apply the vision sensing techniques in highway maneuvering, road geometry models have been utilized and their parameters are estimated to monitor the lane marker locations [5-9].

The lane sensing systems using single camera are effective on planar roadway [5,6], but have limitations in non-planar roadway. In order to extend the lane sensing systems to non-planar road geometry, several schemes with a single camera [7] or a stereo cameras [2,9, *et al.*] are adopted for reconstructing the 3D road structure. In this case, robustness and image processing time become very important from the implementation perspective. For instance, robust vision sensing systems have been developed considering adverse weather condition, poorly structured road, *et al.* [10-12] and speed in image processing time [12,13].

Moreover, the performance of the vision-based lane sensing systems depends on several problems such as; camera specifications, camera configuration, calibration data and lane marker monitoring algorithms. The camera specifications and configuration are determined based on the FOV (Field Of View) and resolution of camera, camera geometry and sensing environment (curvature range, lane marker type, *et al.*). The calibration data can be obtained from the nominal camera configuration [14-16], but lane sensing performance is very sensitive to the reliability of the camera calibration data [17]. The lane marker monitoring algorithms utilize estimation techniques such as Kalman filter [18] and are designed such that their estimation performances are robust with respect to non-planar roadway, speed change and weather conditions. However, the effects of the configuration aspects on the lane sensing performance

This work was supported by grant No. (R01-2003-000-10109-0) from the Basic Research Program of the Korea Science and Engineering Foundation.

Kunsoo Huh is with the School of Mechanical Engineering, Hanyang University, 17 Haengdang-Dong, Sungdong-Ku, Seoul 133-791, Korea (corresponding author to provide phone: 82-2-2290-0437; fax: 82-2-2295-4584; e-mail: khuh2@hanyang.ac.kr).

Jaehak Park, Daegun Hong and Jahng Hyon Park are with the School of Mechanical Engineering, Hanyang University, 17 Haengdang-Dong, Sungdong-Ku, Seoul 133-791, Korea.

Dongil 'Dan' Cho is with the School of Electrical Engineering, Seoul National University, San 56-1, Sinlim-dong, Gwanak-gu, Seoul 151-742 Korea (e-mail: dicho@asri.snu.ac.kr).

are rarely investigated in the literature.

In this paper, a vision-based lane detection system is developed with considering the configuration aspects of vision sensors. With a set of stereo cameras, an inverse perspective mapping method is developed based on the relative calibration between left and right camera coordinates. The correspondence relation between the left and right camera images is included in the coordinate transformations. A new monitoring model for estimating the road geometry parameters is constructed to reduce the number of the measured signals. From the lane sensing perspectives, a selection procedure for the camera specifications and configuration is proposed in this study. Based on the FOV (Field Of View) and lane marker shape, it is shown that appropriate sensing region on the camera image coordinate can be determined. The proposed lane sensing system is implemented on a passenger car with two CCD cameras and its sensing performance is evaluated experimentally while the car is driven on a Korean highway where its curvature is partially known.

II. The Lane Sensing System

The structure of the proposed lane-sensing system consists of stereo cameras, ROI (Region Of Interest) set-up, image processing, inverse mapping and the Kalman filter as shown in Fig. 1. The parallel stereo camera acquires the sequences of road scenes for the left and right image planes. The lane markers inside the selected ROI are detected in the camera coordinate and transformed into the global coordinate through the inverse perspective mapping. Based on the transformed 3D lane markers, the lane geometry model is constructed and its parameters are estimated by the Kalman filter technique [9]. In addition, the lane geometry model is used to predict the ROI locations in the incoming images.

A. Inverse Perspective Mapping

Inverse perspective mapping is an inverse transform from 2D image plane to 3D global coordinate plane. Figure 2 shows the stereo camera coordinate systems used in this study. (X_g, Y_g, Z_g) denotes a global coordinate with its origin represented by projecting the C.G. of the vehicle onto the ground. When the inverse perspective mapping is conducted

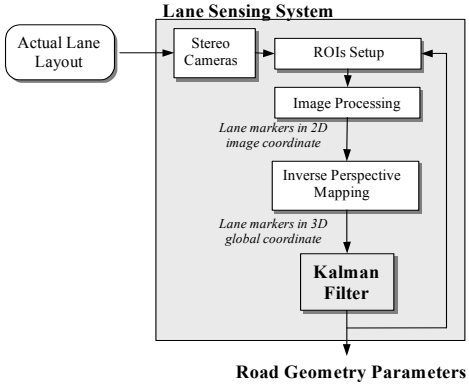

Fig. 1 Structure for the lane sensing system

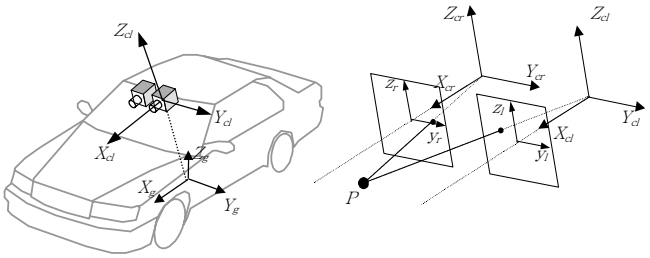

Fig. 2 Coordinate systems

based on the two sequences of images by stereo camera, the correspondence detection that matches the same lane marker in the left and right image is really important. In this study, the well-known epipolar constraint is applied for the correspondence detection using the coordinate rotation matrix (R_{lr}) and translation vector (T_{lr}) between left and right camera coordinates. A point P in the camera coordinates can be projected to the normalized left and right image coordinates using the camera pinhole model.

$$\begin{bmatrix} y_l \\ z_l \end{bmatrix} = \begin{bmatrix} Y_{cl} / X_{cl} \\ Z_{cl} / X_{cl} \end{bmatrix} \tag{1}$$

$$\begin{bmatrix} y_r \\ z_r \end{bmatrix} = \begin{bmatrix} Y_{cr} / X_{cr} \\ Z_{cr} / X_{cr} \end{bmatrix} \tag{2}$$

where (X_{cl}, Y_{cl}, Z_{cl}) and (X_{cr}, Y_{cr}, Z_{cr}) denote the left and right camera coordinates fixed with cameras, respectively. (y_l, z_l) and (y_r, z_r) denote the normalized left and right image coordinates, respectively.

The normalized image coordinate can be transformed to the pixel coordinate based on the intrinsic parameters of a camera.

$$\begin{aligned} y_{pl} &= f_{c1l}(y_l + \alpha_{cl} z_l) + c_{1l} \\ z_{pl} &= f_{c2l} z_l + c_{2l} \end{aligned} \tag{3}$$

$$\begin{aligned} y_{pr} &= f_{c1r}(y_r + \alpha_{cr} z_r) + c_{1r} \\ z_{pr} &= f_{c2r} z_r + c_{2r} \end{aligned} \tag{4}$$

where, y_{pl}, z_{pl} : pixel coordinate of the left camera
y_{pr}, z_{pr} : pixel coordinate of the right camera
f_{c1} : focal length of the y direction in the image plane
f_{c2} : focal length of the z direction in the image plane
α_c : angle between y and z CCD sensor axis
c_1, c_2 : principal point coordinate

Subscripts l and r stand for the left and right camera, respectively. By integrating Eq. (1) through Eq. (4), the pixel coordinate is transformed to the camera coordinate.

$$X_{cl} \begin{bmatrix} 1 \\ y_{pl} \\ z_{pl} \end{bmatrix} = X_{cl} \begin{bmatrix} 1 & 0 & 0 \\ c_{1l} & f_{c1l} & \alpha_{cl} f_{c1l} \\ c_{2l} & 0 & f_{c2l} \end{bmatrix} \begin{bmatrix} 1 \\ Y_{cl} / X_{cl} \\ Z_{cl} / X_{cl} \end{bmatrix} = K_l \begin{bmatrix} X_{cl} \\ Y_{cl} \\ Z_{cl} \end{bmatrix} \tag{5}$$

$$X_{cr}\begin{bmatrix}1\\ y_{pr}\\ z_{pr}\end{bmatrix}=X_{cr}\begin{bmatrix}1 & 0 & 0\\ c_{1r} & f_{c1r} & \alpha_{cr}f_{c1r}\\ c_{2r} & 0 & f_{c2r}\end{bmatrix}\begin{bmatrix}1\\ Y_{cr}/X_{cr}\\ Z_{cr}/X_{cr}\end{bmatrix}=K_r\begin{bmatrix}X_{cr}\\ Y_{cr}\\ Z_{cr}\end{bmatrix} \quad (6)$$

where K_l and K_r are the transformation matrices composed of intrinsic parameters of left and right cameras, respectively. The transformation from the global coordinate to the camera coordinate can be described using the extrinsic parameters of the camera location. In particular, the translation vector and rotation matrix between the left and right cameras are included for the accurate coordinate transformation.

$$\begin{bmatrix}X_{cl}\\ Y_{cl}\\ Z_{cl}\end{bmatrix}=R_{gl}\left(\begin{bmatrix}X_g\\ Y_g\\ Z_g\end{bmatrix}-T_{gl}\right) \quad (7)$$

$$\begin{bmatrix}X_{cr}\\ Y_{cr}\\ Z_{cr}\end{bmatrix}=R_{lr}\left(\begin{bmatrix}X_{cl}\\ Y_{cl}\\ Z_{cl}\end{bmatrix}-T_{lr}\right)=R_{lr}\left(R_{gl}\left(\begin{bmatrix}X_g\\ Y_g\\ Z_g\end{bmatrix}-T_{gl}\right)-T_{lr}\right) \quad (8)$$

where R_{gl} and T_{gl} are the rotation matrix and translation vector, respectively, from the global coordinate to the left camera coordinate. R_{lr} and T_{lr} are the rotation matrix and translation vector, respectively, from the left camera coordinate to the right camera coordinate. By combining Eq. (5) through Eq. (8), the transformation from the global coordinate to the pixel coordinate can be derived.

$$X_{cl}\begin{bmatrix}1\\ y_{pl}\\ z_{pl}\end{bmatrix}=K_lR_{gl}\left(\begin{bmatrix}X_g\\ Y_g\\ Z_g\end{bmatrix}-T_{gl}\right) \quad (9)$$

$$X_{cr}\begin{bmatrix}1\\ y_{pr}\\ z_{pr}\end{bmatrix}=K_rR_{lr}\left(R_{gl}\left(\begin{bmatrix}X_g\\ Y_g\\ Z_g\end{bmatrix}-T_{gl}\right)-T_{lr}\right) \quad (10)$$

The intrinsic and extrinsic parameters of the stereo camera need to be determined through a calibration procedure that will be explained briefly in section 2.3. Finally, the inverse perspective mapping is formulated from the above equations in order to provide the transformation relation from the 2D pixel coordinate to the 3D global coordinate. From the following mapping equation, the camera coordinate values, X_{cr} and X_{cl}, can be also determined.

$$\begin{bmatrix}X_g\\ Y_g\\ Z_g\end{bmatrix}=R_{gl}^{-1}K_l^{-1}\left(X_{cl}\begin{bmatrix}1\\ y_{pl}\\ z_{pl}\end{bmatrix}\right)+T_{gl}=R_{gl}^{-1}\left(R_{lr}^{-1}K_r^{-1}\left(X_{cr}\begin{bmatrix}1\\ y_{pr}\\ z_{pr}\end{bmatrix}\right)+T_{lr}\right)+T_{gl} \quad (11)$$

B. Model-Based Lane Geometry Recognition

Lane geometry has been usually described by a set of polynomial equations [5-9] because their coefficients can be related to the geometry parameters such as curvature, lateral deviation, heading angle, *et al*. For example, constant curvature horizontal roads can be expressed by 2nd order polynomial equations [8]. It is also shown that 3-dimensional lane geometry in highway can be treated as a linear superposition of horizontal and vertical road models. In this study, the horizontal lane geometry is modeled as a 2nd-order polynomial of the longitudinal distance [5] assuming that the horizontal curvature is unknown but slowly time varying.

$$Y_g(X_g)=c_{h0}+c_{h1}X_g+c_{h2}X_g^2/2 \quad (12)$$

where c_{h0} is the lateral offset, c_{h1} is the heading angle and c_{h2} is the horizontal curvature. The vertical lane geometry is also modeled as a 2nd-order polynomial of the longitudinal distance [7] assuming that the vertical curvature is unknown but slowly time-varying.

$$Z_g(X_g)=c_{v0}+c_{v1}X_g+c_{v2}X_g^2/2 \quad (13)$$

where c_{v0} is the variation of camera height, c_{v1} is the tangent of vehicle's pitching angle and c_{v2} is the vertical curvature. The dynamic variations of the parameters in Eq. (12) and Eq. (13) have been considered by differentiating the equations with assuming constant speed [8]. In this case, the parameter estimation requires the measurement of the vehicle motion such as speed and yaw rate.

In this study, based on the fact that horizontal and vertical curvatures are the parameters of main interest and that they are slowly time varying in highway, a constant parameter model is selected for estimating the parameters.

$$\begin{bmatrix}C_{h0}(k+1)\\ C_{h1}(k+1)\\ C_{h2}(k+1)\\ C_{v0}(k+1)\\ C_{v1}(k+1)\\ C_{v2}(k+1)\end{bmatrix}=\begin{bmatrix}1&0&0&0&0&0\\ 0&1&0&0&0&0\\ 0&0&1&0&0&0\\ 0&0&0&1&0&0\\ 0&0&0&0&1&0\\ 0&0&0&0&0&1\end{bmatrix}\begin{bmatrix}C_{h0}(k)\\ C_{h1}(k)\\ C_{h2}(k)\\ C_{v0}(k)\\ C_{v1}(k)\\ C_{v2}(k)\end{bmatrix} \quad (14)$$

The above model doesn't need any motion data except the image sequence and its real-time computation burden is decreased due to the simplicity of the model. Based on the above equation, Kalman filter [18] is designed for estimating the parameters. The center of the next ROIs is predicted based on the estimated lane parameters, because the lane markers appear in the limited region of the road images.

III. Vision Sensor Configuration

A. Lane Characteristics

Vision sensor configuration can be classified into two

issues: camera specifications such as focal length, resolution, pixel size, *et al*. and camera geometry such as camera height, tilting angle, *et al*. Based on the lane characteristics of Korean highway as shown in Table 1, a selection rule of the sensor configuration is investigated in this section.

B. FOV (Field of View)

In general, FOV (Field Of View) of vision sensors in real space can be determined based on camera geometry as shown in Fig. 3. The horizontal FOV of vision sensors is related to the width parameters, w_1 and w_2, whereas the vertical FOV of vision sensors is dependent on the distance parameters, d_1 and d_2. Based on the geometrical relations as illustrated in Fig. 3, the width and distance parameters can be described as follows.

$$d_v(k) = h_c \cdot \tan\left[\left(\frac{\pi}{2} - \beta\right) - \left(\frac{\alpha_v}{2} - k \cdot \frac{\alpha_v}{n_v}\right)\right]$$

$$w_v(k) = 2 \cdot \sqrt{d^2(k) + h_c^2} \cdot \tan\left(\frac{\alpha_h}{2}\right), \quad \text{where } k = 1 \sim n_v \qquad (15)$$

$$\Rightarrow \begin{cases} d_v(k) = d_1, \ w_v(k) = w_1, & when \quad k = 0 \\ d_v(k) = d_2, \ w_v(k) = w_2, & when \quad k = n_v \end{cases}$$

where h_c and β are the height and tilting angle of the camera, respectively. The horizontal and vertical camera angles, α_h and α_v, can be obtained from the camera specifications.

$$\alpha_h = 2 \cdot \tan^{-1}\left(\frac{hCCD \times n_h}{2} \cdot \frac{1}{f}\right)$$

$$\alpha_v = 2 \cdot \tan^{-1}\left(\frac{vCCD \times n_v}{2} \cdot \frac{1}{f}\right) \qquad (16)$$

where *hCCD* and *vCCD* indicate the size of horizontal and vertical camera pixel, respectively. n_h and n_v indicate the number of horizontal and vertical camera pixels, respectively. f is the focal length of camera given by the manufacturer.

For the vision-based lane detection, design specification for the FOV can be obtained based on the lane characteristics of highway as listed in Table 1. The maximum value for the horizontal FOV is related to the lane width, L_{wi}, and the horizontal offset, h_{offset}, due to the curvature of curved roads. The maximum value for the vertical FOV is calculated by the lane length and gap of dashed lines.

$$w_{\max} = (2 \cdot L_{wi} + h_{offset}) \cdot (1 + \varepsilon_h)$$

$$d_{\max} = (L_l + L_g) \cdot (1 + \varepsilon_v) \qquad (17)$$

where w_{max} and d_{max} are the maximum width and distance of the FOV for the effective lane sensing. ε_h and ε_v are the sensing error in the horizontal and vertical directions, respectively.

TABLE 1 HIGHWAY CHARACTERISTICS (SPEED LIMIT: 100 KPH)

maximun curvature (1/m)	horizontal		1/460
	vertical		4/100
minimum lane width: L_{wi} (m)			3.5
lane marker shape.	solid lane	thickness: L_{th} (m)	0.1~0.15
	dashed lane	length: L_l (m)	10
		gap: L_g (m)	10
		thickness: L_{th} (m)	0.1~0.15

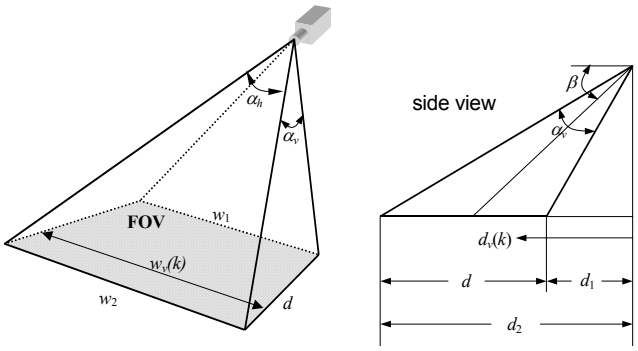

Fig. 3 FOV defined from camera geometry

C. Resolution

For the lane detection performance, resolution problem is considered for the horizontal and vertical directions. In particular, the horizontal spatial resolution is defined as the physical length per horizontal pixel. The horizontal resolution can have different values because the horizontal FOV of Eq. (15) varies depending on the vertical position in the image.

$$Rh_s(k) = w_v(k) / Rh_i \qquad (18)$$

where Rh_i : horizontal image resolution

$Rh_s(k)$: horizontal spatial resolution at vertical position k

The horizontal image resolution means the number of row pixels in the image plane. The span pixel in the horizontal direction represents the number of pixels spanning the smallest feature such as lane thickness and can be expressed using the horizontal spatial resolution of Eq. (18).

$$F_p(k) = R_f / Rh_s(k) \qquad (19)$$

where R_f is the feature resolution and means the smallest feature detected reliably by vision sensors. In general, the span pixel, F_p, should be more than five pixels considering the image filtering.

D. Determination of Vision Sensor Configurations

The camera specifications and configurations are determined for the lane detection vision sensors. The selected camera is Sony XC-55 and its specifications are

listed in Table 2 where the image resolution is *640×480* pixels and the focal length of *16 mm*. The stereo camera is installed with the height of *1.2 m* and the tilting angel of *5°*. In this case, the width of the FOV is calculated using Eq. (15) with respect to the vertical location (pixel) of the image plane and is illustrated in Fig. 4. Based on Eq. (17) and the sensing error of *10%*, the maximum size of the FOV in the horizontal and vertical directions is calculated and its values are *9m* and *22m*, respectively. Because the minimum horizontal FOV should be greater than the lane width (3.5m), the appropriate sensing region in the image plane can be determined from Fig. 4 and should be the vertical range between 200^{th} and 350^{th} pixels.

The determined sensing region is also appropriate from the perspective of the distance variation because the distance around the 350^{th} pixel in the vertical location of Fig. 5 is equivalent to the vertical FOV size of *26m (= 32m - 6m)*. By assuming that the feature resolution in Eq. (19) is the lane thickness given in Table 1, the span pixel variation can be calculated and is shown in Fig 6. The sensing region determined from Fig. 4 provides *7-19* span pixels which are sufficient for detecting the lane markers.

IV. Real-Time Sensing Experiment

A. Hardware and Software for Experiment

In order to verify the proposed lane sensing algorithm, stereo vision system is installed on a passenger car as shown Fig. 7. Two CCD cameras are mounted in parallel and can acquire images at the rate of 30 fps (Frames/sec) by a progressive scan manner. Image sequences from the two CCD cameras are transferred to PC memory through a frame grabber (Matrox meteor II-MC). The lane sensing software has been developed with C++ language and the Intel OpenCV library.

TABLE 2 CAMERA SPECIFICATIONS (SONY XC-55)

Image resolution	horizontal	640 pixels
	vertical	480 pixels
Pixel size	horizontal (hCCD)	0.0074 mm
	vertical (vCCD)	0.0074 mm
Focal length		16 mm

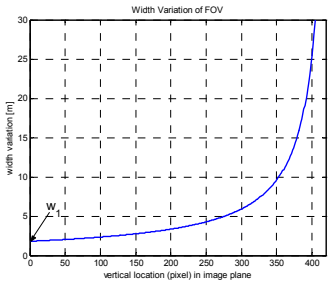

Fig. 4 Width variation of horizontal FOV

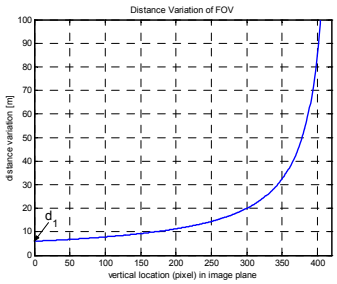

Fig. 5 Distance variation of vertical FOV

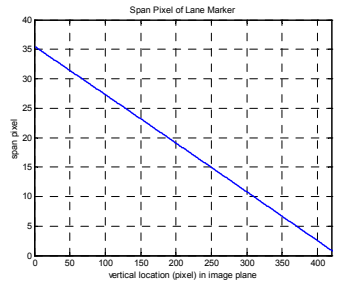

Fig. 6 Span pixel variation for detecting lane markers

Fig. 7 Stereo Camera Set-up

B. Lane Detection and ROI Setup

Detection of the initial lane shape from the first image is a difficult task without driver's help. In this study, a template matching method with image segmentation is applied to the noise-filtered and edge-detected image. As shown Fig. 8, a matching test is carried out starting from the left-bottom part of the left image because the bottom part has the best spatial resolution in the image plane. Once a proper lane marker is detected, the matching test is continued in the longitudinal direction in order to verify the detected lane marker and to find other line segments. After the left lane is extracted successively, the position of the right lane markers can be easily predicted in the same image using the lane width information. The same procedure is conducted on the right image to find the left and right lane markers and the results are evaluated considering the geometry constraints of parallel stereo camera. However, there is no need to repeat this procedure after the initial lane shape is detected. Based on the initial lane markers and the characteristics of highway, location of the ROIs for the upcoming lane markers can be approximately expected.

C. Experimental Results

The sensing performance is evaluated experimentally while the car with the lane sensing system is driven on a portion of Korean highways. The test road consists of right turning, straight and left turning flat roadway and its horizontal curvature is known. The lane parameters in Eq. (12) and Eq. (13) are estimated based on the proposed method in section 2.2. Figure 9 and Fig. 10 show the estimation results of horizontal curvature and vertical curvature, respectively. The estimated horizontal curvature follows the real value pretty well and the estimated vertical curvature is very small due to the flat roadway.

V. Conclusions

A lane detection system with stereo camera is proposed with considering the configuration aspects. The inverse perspective mapping method is developed by including the transformation between the left and right coordinates. A simplified road geometry model is utilized for reducing the number of the measured signals and the processing time. The varying property of the horizontal FOV (Field of View) is derived and the camera configuration aspects such as resolution and span pixel are expressed using the property. The maximum FOV in the horizontal and vertical directions are selected using the highway characteristics. The appropriate sensing range in the image plane is determined based on the width variation curve. The proposed lane detection system is installed in a passenger car and its lane detection performance such as the horizontal curvature estimation coincides well with the real value of the highway.

References

[1] Taylor, C.J., Malik, J. and Weber, J., "A Real-Time approach to Stereopsis and Lane-Finding," Proc. IEEE Intelligent Vehicles Symposium, 1996, pp. 207-212.

[2] Bertozzi, M. and Broggi, A., "GOLD: A Parallel Real-Time Stereo Vision System for Generic Obstacle and Lane Detection," IEEE Transactions on Image Processing, Vol. 7, No. 1, 1998, pp. 62-81.

[3] Pomerleau, D., "RALPH: Rapidly Adapting Lateral Position Handler," Proc. the IEEE Intelligent Vehicles Symposium, 1995, pp. 506-511.

[4] Cerone, V., Bertozzi, M. and Broggi, A., "Experimental Results in Vision–based Lane Keeping for Highway Vehicles," Proceedings of the American Control Conference, 2002, pp. 869-874.

[5] Takahashi, A. and Ninomiya, Y., "Model-Based lane recognition," Proc. IEEE Intelligent Vehicles Symposium, 1996, pp. 162-166.

[6] Goldbeck , J. and Huertgen, B., "Lane Detection and Tracking by Video Sensors," IEEE International Conference on Intelligent Transportation Systems, 1999, pp. 74-79.

[7] Dickmanns, E.D. and Mysliwetz, B.D., "Recursive 3-D road and relative ego-state recognition," IEEE Trans. on PAMI, Vol. 14, No. 2, 1992, pp. 199-213.

[8] Lin, C.F. and Ulsoy, A.G., "Lane Geometry Reconstruction: Least Square Curve Fit Versus Kalman Filter," ASME Advanced Automotive Technologies, DSC-Vol.56/DE-Vol. 86, 1995, pp. 63-70.

[9] Huh, K. and Park, Y., "Development of a robust lane sensing system using vision sensors," Proceeding of AVEC, 2002, pp. 769-774.

[10] Gern, A., Moebus, R. and Frank, U., "Vision-based Lane Recognition under Adverse Weather Conditions Using Optical Flow," Proc. IEEE Intelligent Vehicles Symposium, 2002, pp. 652-657.

[11] Gehrig, S. K., Gern, A., Heinrich, S. and Woltermann, B., "Lane Recognition on Poorly Structured Roads-the Bots Dot Problem in California," IEEE 5th International Conference on Intelligent Transportation Systems, 2002, pp.67-71.

[12] Aufrére, R., Chapuis, R. and Chausse, F., "A fast and robust vision based road following algorithm," Proc. IEEE Intelligent Vehicles Symposium, 2000, pp. 192-197.

[13] González, J. P. and Özzgüner, Ü., "Lane Detection Using Histogram-Based Segmentation and Decision Trees," Proc. IEEE Intelligent Transportation Systems, 2000, pp. 346-351.

[14] Zhang, Z., "Flexible Camera Calibration By Viewing a Plane From Unknown Orientations," 7th IEEE International Conference on Computer Vision, 1999, pp. 666-673.

[15] Heikkilä, J. and Silvén, O., "Calibration Procedure for Short Focal Length Off-the shelf CCD cameras," Proc. 13th International Conference on Pattern Recognition, 1996, pp. 166-170.

[16] Heikkilä, J. and Silvén, O., "A Four-step Camera Calibration Procedure with Implicit Image Correction," IEEE computer society computer vision and pattern recognition conference, 1997, pp 1106-1112.

[17] Ernst, S., Stiller, C., Goldbeck, J. and Roessig, C., "Camera calibration for lane and obstacle detection," IEEE International Conference on Intelligent Transportation Systems, 1999, pp. 356-361

[18] Grewal, M.S. and Andrews, A.P., Kalman Filtering Theory and Practice, Prentice Hall, 1993.

Fig. 8 Initial Lane Searching from the edge-detected image

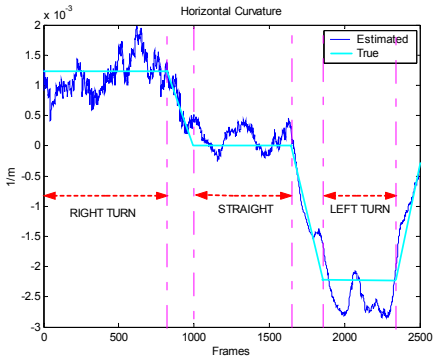

Fig. 9 Horizontal curvature from experiments

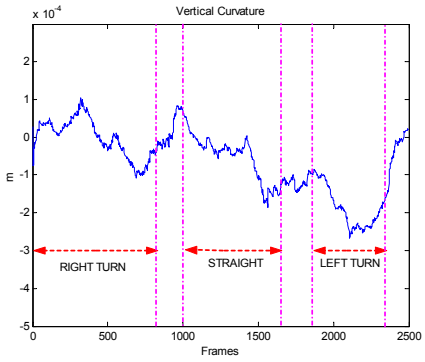

Fig.10 Vertical curvature from experiments